Determination of nonlinear refractive index of large area monolayer MoS2 at telecommunication wavelength using time-resolved Z-scan technique

Determination of nonlinear refractive index of large area monolayer MoS_2 at telecommunication wavelength using time-resolved Z-scan technique

Jing Wen Chew[*], Wu Yi Chong[†,§], Sithi Vinayakam Muniandy[*], Yuen Kiat Yap[†,‡] and Harith Ahmad[†]

[†]Photonics Research Centre, University of Malaya,
50603 Kuala Lumpur, Malaysia

[*]Department of Physics, Faculty of Science, University of Malaya,
50603 Kuala Lumpur, Malaysia

[‡]Heriot-Watt University Malaysia, Precinct 5,
62200 Putrajaya, Malaysia

[§]wuyi@um.edu.my

Received (Day Month Year)
Accepted (Day Month Year)
Published (Day Month Year)

The nonlinear refractive index of large area monolayer molybdenum disulphide (MoS_2) thin film at the 1550 nm wavelength band is determined using time resolved z-scan technique. MoS_2 exhibits positive nonlinear phase shift with a large nonlinear refractive index, n_2 value of 1.40×10^{-13} m^2 W^{-1}. The obtained value is similar to the n_2 value of monolayer MoS_2 film measured at 2.0 μm, and is approximately 5 and 7 orders of magnitude larger than silicon and common bulk dielectrics. The large n_2 indicates that MoS_2 can be used as nonlinear refractive 2D material for photonics applications operating in the 1550 nm optical telecommunications wavelength band.

Keywords: nonlinear refractive index; molybdenum disulphide; Z-Scan; telecommunication wavelength

1. Introduction

The successful exfoliation of atomically thin graphene sheets at the turn of the 21st century has kick-started a new research field on two-dimensional (2D) materials.[1] It is found that monolayer or few-layer graphene exhibit excellent electronic and optical properties that is not present in its bulk form.[2] Since then, rapid progress has been made in the development and characterization of new families of 2D materials such as hexagonal boron nitride,

transition metal dichalcogenides (TMDs) and black phosphorus.[3-5] Their unique properties have opened up the possibilities of new applications in nanoscale electronics, photonics sensing and signal processing when integrated with silicon complementary metal-oxide-semiconductor and optical waveguide platforms.[6]

In the photonics field, the nonlinear optical (NLO) properties of 2D materials are widely studied. They exist in two distinct forms: 1) nano- and micro-flakes dispersed in solution, and 2) uniform single- or few-layer thin film with large coverage area, depending on the methods of fabrication.[7] Their NLO properties play an important role in pulsed laser generation, all-optical switching, frequency conversion applications, etc. In particular, a monolayer molybdenum disulphide (MoS_2) is found to have the ability to produce pulsed lasers due to its saturable absorption characteristic.[8-12] NLO properties in the visible and near infrared wavelengths are normally studied using Z-scan technique.[9, 13-16] Wang et al.[17] investigated the n_2 of liquid-phase-exfoliated MoS_2 nano-flakes dispersion in the wavelength of 532 nm and 1064 nm using Z-scan technique. Wu et al.[18] provided a comprehensive study of the third order nonlinear susceptibility ($\chi^{(3)}$) of MoS_2 nano-flakes dispersed solution in a wide wavelength range from 473 nm to 830 nm using spatial self-phase modulation method. More recently, the n_2 of few-layer MoS_2 thin film – grown using chemical vapour deposition (CVD) – was investigated using four-wave mixing method at 1550 nm[19]. The studies above were carried out on few-layer MoS_2 with flake size of not larger than 500 μm in size. However, with the advent of MoS_2 fabrication and transfer techniques, large-area MoS_2 thin films are made available on optical substrates such as silica and polymers.[3, 20] It would be interesting to study the NLO properties of large-area monolayer MoS_2 as it is expected to provide a more accurate NLO response compared to dispersed MoS_2 flakes. Despite this, there is no report on the study of the NLO properties of large area monolayer MoS_2 thin film using Z-scan technique at the 1550 nm telecommunication wavelength band.

In this work, we investigate the third order nonlinearities of large area monolayer MoS_2 thin film using time-resolved Z-scan technique and determine the value of n_2. We compare the value of n_2 obtained from large area monolayer MoS_2 film with silicon and other common bulk dielectric materials. This result would encourage more development of nonlinear photonics applications, such as all-optical switching and wavelength conversion that operate in the 1550 nm optical telecommunication wavelength band.

2. Methods

2.1. Characterization of atomically thin MoS_2

A CVD-grown monolayer MoS_2 thin film on a polydimethylsiloxane (PDMS) substrate is purchased from 6Carbon Technology. The monolayer MoS_2 thin film has a coverage area of 1 cm × 1 cm. Figure 1 shows the optical micrograph of the sample. In Fig. 1(a), it can be seen that there is an optical contrast between the MoS_2 thin film and the PDMS substrate, which allows one to visually determine the position of the film on the substrate. Besides, from Fig. 1(b), it can be inferred that the deposited MoS_2 forms good coverage on the substrate, which will ensure good overlapping of MoS_2 sample with the incident laser beam during the Z-scan measurement. Atomic force microscopy (AFM) is carried out using NT-MDT with semi-contact mode to measure the thickness of the MoS_2 film. From Fig. 1(c), the apparent height measured is ~ 0.8 nm, which indicates the monolayer thickness of the MoS_2 film.[21]

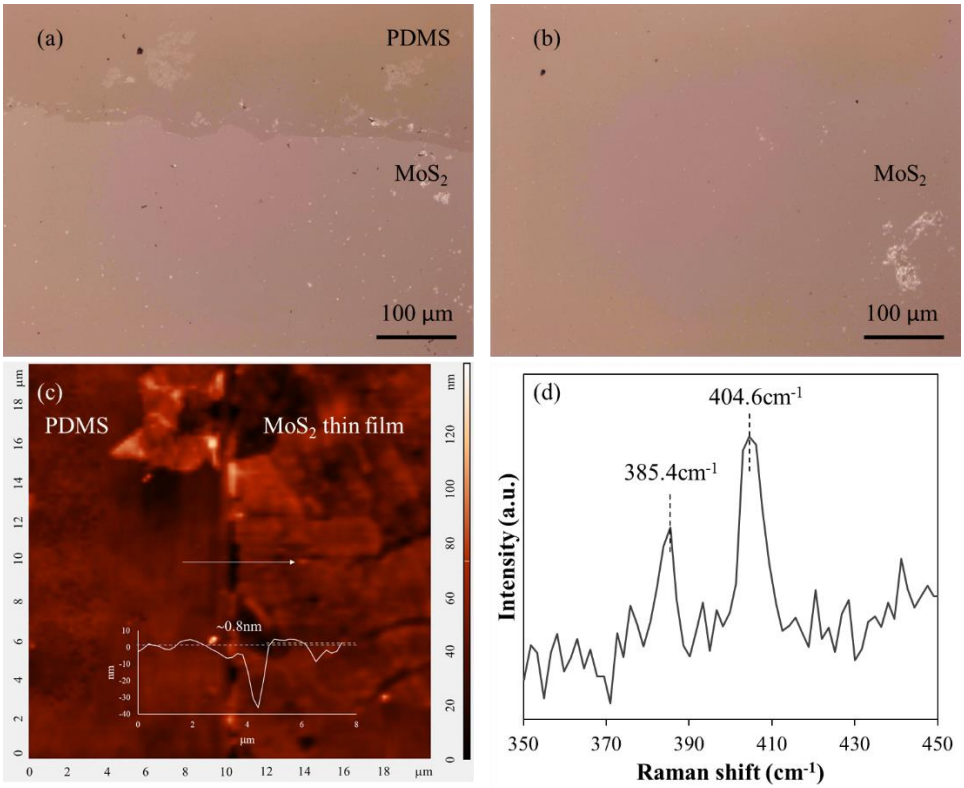

Fig.1. Optical micrographs of MoS_2 sample: (a) boundary of the MoS_2 deposition; (b) continuous layer of the grown MoS_2; (c) AFM image of MoS_2 on PDMS; (d) Raman spectrum of MoS_2 sample with 532 nm excitation wavelength.

Raman spectroscopy is carried out on the sample using Renishaw InVia micro-Raman spectrometer. The wavelength of the Raman laser source is 532 nm with an excitation power of 0.25 mW. The power used is kept low to avoid optical damage to the sample. From Fig. 1(d), two characteristic peaks of 385.4 cm^{-1} and 404.6 cm^{-1} are observed, which correspond to the in-plane E_{2g} and out-of-plane A_{1g} modes of monolayer MoS_2, respectively. Both of these vibrational modes are thickness dependent. As the number of layers reduces from bulk to monolayer, the E_{2g} and A_{1g} modes will experience red- and blue-shifts, respectively. This is mainly due to the change in stacking structure of individual MoS_2 sheets, which in turn changes the atomic vibration of these modes.[22, 23] This would provide another quantitative measure to determine the number of layers of the MoS_2 film. We perform Raman spectroscopy on eight locations, with most of the spectra resembled the result in Fig. 1(d). The values of E_{2g} and A_{1g} modes obtained are consistent with single layer MoS_2.

2.2. Measurement of nonlinear optical (NLO) properties

A time-resolved Z-scan technique is employed to determine the NLO properties of the sample.[24-26] It is typically used to solve the cumulative thermal effect in the sample when a high repetition rate laser is used as the laser source in Z-scan measurement. The

experimental setup is illustrated in Fig. 2. A mode-locked fiber laser with a center wavelength of 1560 nm, laser repetition rate of 1.0 MHz and pulse width of 450 fs is used as the laser source. An optical attenuator is used to vary the laser power. The beam is expanded by a factor of 10 using a pair of positive convex lenses (L_1 and L_2) in Keplerian beam expanding configuration. A mechanical shutter is placed at the focal point of L_1 to create an opening window of 5 ms with risetime of 30 µs. The laser beam is focused by L_3 (f = 100 mm) to a beam waist radius of ω_0 = 26 µm and Rayleigh length, z_0 = 1.4 mm. Two identical photodiodes (PDs) are used to measure the signal powers. PD_1 receive the near field open-aperture (OA) signal while PD_2 measures the far-field closed-aperture (CA) signal. The CA Z-Scan is performed at 20 % aperture transmission. The sample is translated along the laser axis using a linear translation stage. The intensity, I_o, of the pulse laser used in time-resolved Z-scan measurement is 6.2 GW cm^{-2}. Each measurement is repeated 3 times.

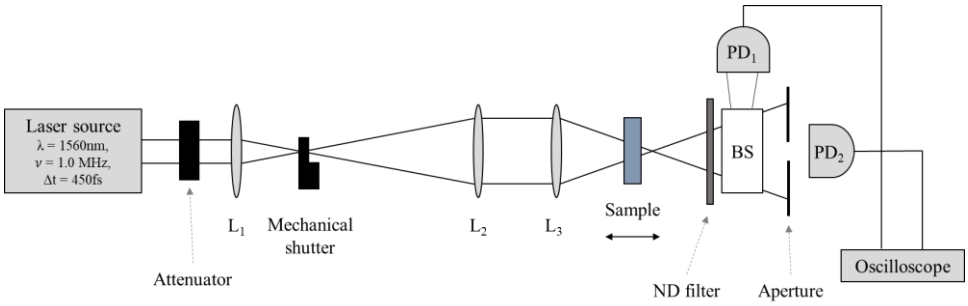

Fig. 2. Experimental setup of the time-resolved Z-scan technique. L_1, L_2 and L_3 are plano-convex lenses. BS is a beam splitter. PD_1 and PD_2 are photodiodes which measure the open-aperture and far-field closed-aperture signal respectively.

3. Results and discussion

The normalized signal intensity in a time-resolved Z-scan CA measurement can be described using the Falconieri model below:[24]

$$\frac{I(\zeta,t)}{I(\zeta,0)} = 1 + \frac{\vartheta(q)}{q}\frac{1}{(1+\zeta^2)^{q-1}}\tan^{-1}\left(\frac{2q\zeta}{[p^2+\zeta^2]\frac{t_c(\zeta)}{2qt}+p+\zeta^2}\right), \qquad (3.1)$$

where q is the order of absorption, ϑ is the thermal lens strength, $\zeta = z/z_0$ is the normalized z-position, $p = 2q + 1$ and t_c is the characteristic time of the material. The parameter t represents the time when the mechanical shutter is turned on.

Eq. (3.1) demonstrate the change in normalized CA signal intensity due to the thermal lensing effect as a function of ζ and t. The thermal lensing effect takes place when $t > 0$, therefore it is possible to determine the instantaneous electronic nonlinearity (related to n_2) at $t = 0$. In other words, the two optical effects can be separated using Eq. (3.1).[24]

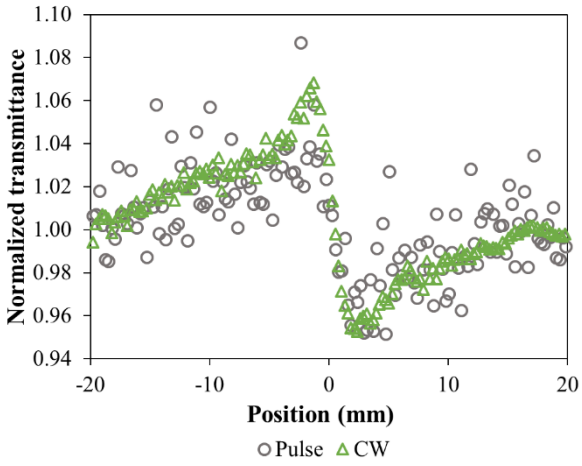

Fig. 3. Conventional Z-scan measurements upon MoS_2 sample using pulse and CW laser sources. The average power of both laser sources is 3 mW. Similar CA trend between pulse and CW laser sources imply that the observed lensing properties originates from cumulative thermal effect.

To obtain the q value in Eq. (3.1), conventional Z-scan measurements are performed on the MoS_2/PDMS sample using both pulsed and continuous wave (CW) laser sources. Since the intensity of the CW laser is low (< 1 kW/cm^2), we do not expect to see nonlinear refraction (NLR) during the CA measurement. However, we found that at the same average power levels, both traces show self-defocusing characteristics, i.e. a peak-to-valley profile as shown in Fig. 3. The normalized peak-valley transmittance difference (ΔT_{p-v}) obtained using both laser sources also show a similar value, which is ~ 0.11. This implies that the self-defocusing properties originate from the cumulative thermal effect in the sample. Besides that, the normalized peak-valley distance (ΔS_{p-v}) is determined to be $3.7z_0$. This value is close to the theoretical value of $3.46z_0$ that corresponds to one photon absorption thermal lensing effect.[24] Therefore, we set q = 1 in the following time-resolved Z-scan analysis, and Eq. (3.1) can be reduced to:

$$\frac{I(\zeta,t)}{I(\zeta,0)} = 1 + \vartheta(1)\tan^{-1}\left(\frac{2\zeta}{[9+\zeta^2]\frac{t_c(\zeta)}{2t}+3+\zeta^2}\right), \qquad (3.2)$$

Figure 4 demonstrates two normalized transmittance traces of the MoS_2/PDMS sample over a period of 2 ms. These traces correspond to the normalized transmittance at the pre-focal and post-focal z-position. It can be seen from this figure that there is a discernible change in the normalized transmittance before and after 0.45 ms, inferring that there is an inversion of peak and valley of the CA curve. The pre-focal z-scan signal changes from a valley to a peak, so does the post-focal z-scan signal. This implies that the instantaneous electronic nonlinearity and thermal lensing effect of MoS_2/PDMS sample have opposite signs.

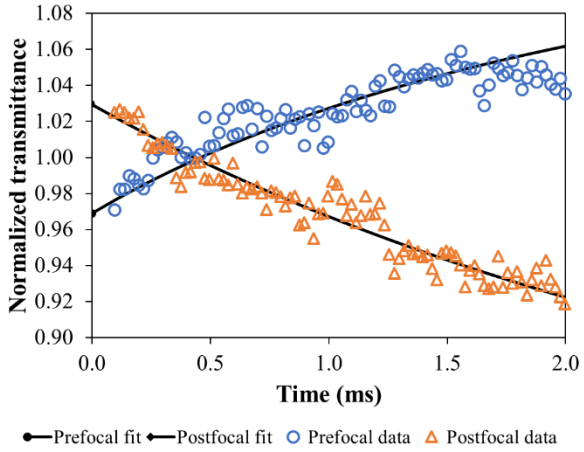

Fig. 4. Normalized transmittance trace of MoS_2 sample measured at pre-focal and post-focal z-positions. The solid curves are the fitting curves generated from Eq. (3.2). The open symbols represent the experimental data, while the solid symbols are the extrapolated values at t = 0 which will be used to reconstruct the Z-scan profile.

Figure 5 represents the reconstructed CA Z-scan profiles of MoS_2/PDMS sample at t = 0 and 2 ms. As previously suggested, it can be observed that at t = 0, the sample presents a NLR with self-focusing characteristic. The ΔS_{p-v} for the NLR trace is calculated to be $1.80z_0$, which is close to the theoretical value of $1.72z_0$ for Kerr induced self-focusing (without thermal lensing). At t = 2 ms, the sample exhibits self-defocusing thermal lensing characteristic. It should be noted that at this intensity, we do not observe NLA such as saturable absorption from the MoS_2 from the OA Z-scan measurement (see Fig. 5 inset). This is probably due to the fact that the linear absorption of the monolayer MoS_2 is ~ 0.2%, which is less than the 1% measurement sensitivity of our current measurement setup. Nevertheless, the possibility of the presence of NLA cannot be omitted totally, as it could exist within the noise level.

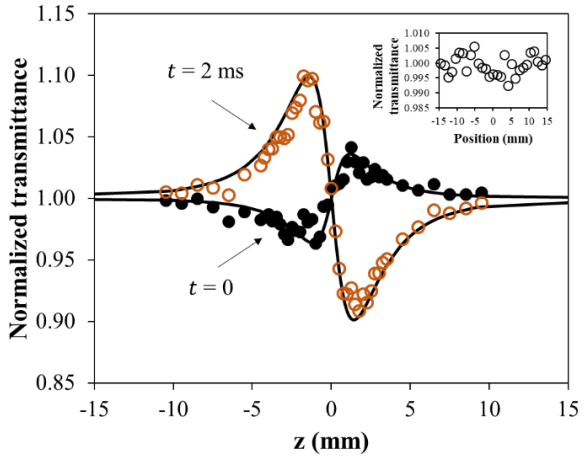

Fig. 5. Reconstructed Z-scan profiles of MoS_2/PDMS sample at t = 0 and 2 ms. The solid line traces are corresponding theoretical fit. Inset: OA Z-scan trace of MoS_2, in which no significant NLA can be observed.

From Fig. 5, the normalized transmittance of CA Z-scan at t = 0 can be fitted using Sheik-Bahae et al.[27] model below:

$$T(z, \Delta\Phi_0) \simeq 1 - \frac{4\Delta\Phi_0\zeta}{(\zeta^2+9)(\zeta^2+1)}, \qquad (3.3)$$

where $T(z, \Delta\Phi_0)$ is the normalized transmittance, $\Delta\Phi_0 = kn_2I_0L_{eff}$ is the on-axis phase shift at the laser focal point, and $\zeta = {}^{z}/_{z_0}$, with z_0 the Rayleigh length. The model fits the experimental data well as shown in Fig. 5 and enable us to relate the n_2 with $\Delta\Phi_0$ using

$$n_2 = \frac{\Delta\Phi_0}{kI_0L_{eff}}, \qquad (3.4)$$

with $k = 2\pi/\lambda$, where λ is the wavelength of laser, and $L_{eff} = 1 - e^{-\alpha L}/\alpha$, with L the thickness of the sample, where $L = L_{MoS_2} + L_{PDMS}$. and α the linear absorption coefficient of the sample. The linear absorption coefficient of the sample at 1550 nm is approximately 2.0 cm^{-1}. Using Eq. (3.4), we have calculated the n_2 of MoS_2/PDMS sample to be 1.49 × 10^{-18} m^2 W^{-1}. However, the measured n_2 refers to the effective n_2 of the sample, which consists of the monolayer MoS_2 and the PDMS substrate. Based on Eq. (3.4), the n_2 obtained from the experiment is evaluated from the on-axis phase shift $\Delta\Phi_0 = kn_2I_0L_{eff}$. Consider the NLR from the PDMS substrate, we can rewrite the $\Delta\Phi_0$ as $\Delta\Phi_0 = kI_0(n_{2,MoS_2}L_{MoS_2} + n_{2,PDMS}L_{PDMS})$. In this way, the n_{2,MoS_2} can be obtained from the equation below:

$$n_{2,MoS_2} = \frac{n_2L_{eff} - n_{2,PDMS}L_{PDMS}}{L_{MoS_2}}, \qquad (3.5)$$

where L_{MoS_2} is 0.7 nm, L_{PDMS} is 500 μm, and n_2 = 1.49 × 10^{-18} m^2 W^{-1}. To determine the contribution of n_2 from PDMS substrate, time-resolved Z-scan is also carried out on a clean PDMS substrate without MoS_2 thin film coating. Our result shows that PDMS possesses a $n_{2,PDMS}$ value of 1.22 × 10^{-18} m^2 W^{-1}. Using Eq. (3.5), the value of n_{2,MoS_2} can be deduced to be 1.40 × 10^{-13} m^2 W^{-1}. This value is similar to the n_2 value of monolayer MoS_2 measured at 2.0 μm, which is 2.5 × 10^{-13} m^2 W^{-1}.[12] In addition, it is approximately 5[28-30] and 7[31, 32] orders of magnitude larger than that of the silicon and bulk dielectric materials, respectively, making it an potential 2D material for the development of optical nonlinear devices operating in the 1550 nm telecommunication wavelength range.

4. Conclusion

The nonlinear optical properties of large-area monolayer MoS_2 in the 1550 nm wavelength band is successfully determined using time-resolved Z-scan technique. We found that the MoS_2 has a nonlinear refractive index, n_2 = 1.40 × 10^{-13} m^2 W^{-1}, which is approximately 5 and 7 orders of magnitude larger than the value of silicon and other common bulk dielectrics, respectively. The obtained value is also similar to the value measured at 2.0 μm. This suggests that MoS_2 is a potential 2D material for nonlinear optics application such as in all-optical switching operating in the optical telecommunication wavelength region.

Acknowledgements

The work is supported by the Malaysian Ministry of Higher Education Fundamental Research Grant Scheme (FRGS/1/2020/STG07/UM/01/2). The PhD studies undertaken by J.W. Chew is supported by Malaysia's Ministry of Education via MyBrainSc scholarship.

References

1. Novoselov K. S., Geim A. K., Morozov S. V., Jiang D., Zhang Y., Dubonos S. V., Grigorieva I. V. and Firsov A. A., Electric field effect in atomically thin carbon films, *Science* **306** (2004) 666-669.
2. Xia F., Wang H., Xiao D., Dubey M. and Ramasubramaniam A., Two-dimensional material nanophotonics, *Nature Photonics* **8** (2014) 899.
3. Manzeli S., Ovchinnikov D., Pasquier D., Yazyev O. V. and Kis A., 2D transition metal dichalcogenides, *Nature Reviews Materials* **2** (2017) 17033.
4. Balla N. K., O'brien M., McEvoy N., Duesberg G. S., Rigneault H., Brasselet S. and McCloskey D., Effects of excitonic resonance on second and third order nonlinear scattering from few-layer MoS2, *ACS photonics* **5** (2018) 1235-1240.
5. Wang X. and Lan S., Optical properties of black phosphorus, *Advances in Optics and Photonics* **8** (2016) 618-655.
6. Sun Z., Martinez A. and Wang F., Optical modulators with 2D layered materials, *Nature Photonics* **10** (2016) 227-238.
7. You J., Bongu S., Bao Q. and Panoiu N., Nonlinear optical properties and applications of 2D materials: theoretical and experimental aspects, *Nanophotonics* **8** (2019) 63-97.
8. Woodward R., Kelleher E., Howe R., Hu G., Torrisi F., Hasan T., Popov S. and Taylor J., Tunable Q-switched fiber laser based on saturable edge-state absorption in few-layer molybdenum disulfide (MoS 2), *Optics express* **22** (2014) 31113-31122.
9. Zhang H., Lu S., Zheng J., Du J., Wen S., Tang D. and Loh K., Molybdenum disulfide (MoS 2) as a broadband saturable absorber for ultra-fast photonics, *Optics express* **22** (2014) 7249-7260.
10. Du J., Wang Q., Jiang G., Xu C., Zhao C., Xiang Y., Chen Y., Wen S. and Zhang H., Ytterbium-doped fiber laser passively mode locked by few-layer Molybdenum Disulfide (MoS 2) saturable absorber functioned with evanescent field interaction, *Scientific reports* **4** (2014) 6346.
11. Chong W., Yap Y., Behameen S. and Ahmad H., Study of a high output coupling ratio Q-switched erbium-doped fibre laser using MoS2 saturable absorber, *Laser Physics* **27** (2017) 025104.
12. Pan H., Chu H., Pan Z., Zhao S., Yang M., Chai J., Wang S., Chi D. and Li D., Large-scale monolayer molybdenum disulfide (MoS2) for mid-infrared photonics, *Nanophotonics* **9** (2020) 4703-4710.
13. Demetriou G., Bookey H. T., Biancalana F., Abraham E., Wang Y., Ji W. and Kar A. K., Nonlinear optical properties of multilayer graphene in the infrared, *Optics express* **24** (2016) 13033-13043.
14. Lu H. and Gu B., Synthesis, characterization, and femtosecond third-order optical nonlinearity of Au@ Ag core–shell nanoparticles, *Journal of Nonlinear Optical Physics & Materials* **31** (2022) 2250002.
15. Liu Z., Wu F., Zhang S., Liu C. and Zeng X., Nonlinear optical properties of the tartrazine, *Journal of Nonlinear Optical Physics & Materials* (2022) 2350014.

16. Rudenko V., Liakhovetskyi V., Dovbeshko G., Brodin A., Romanyuk V. and Juškėnas R., Nonlinear optical properties of graphene and pyrolytic carbon: A comparative study, *Journal of Nonlinear Optical Physics & Materials* **28** (2019) 1950016.
17. Wang K., Feng Y., Chang C., Zhan J., Wang C., Zhao Q., Coleman J. N., Zhang L., Blau W. J. and Wang J., Broadband ultrafast nonlinear absorption and nonlinear refraction of layered molybdenum dichalcogenide semiconductors, *Nanoscale* **6** (2014) 10530-10535.
18. Wu Y., Wu Q., Sun F., Cheng C., Meng S. and Zhao J., Emergence of electron coherence and two-color all-optical switching in MoS2 based on spatial self-phase modulation, *Proceedings of the National Academy of Sciences* **112** (2015) 11800-11805.
19. Zhang Y., Tao L., Yi D., Xu J.-B. and Tsang H. K., Enhanced four-wave mixing with MoS2 on a silicon waveguide, *Journal of Optics* **22** (2020) 025503.
20. Castellanos-Gomez A., Buscema M., Molenaar R., Singh V., Janssen L., Van derZant H. S. and Steele G. A., Deterministic transfer of two-dimensional materials by all-dry viscoelastic stamping, *2D Materials* **1** (2014)
21. Luo S., Cullen C. P., Guo G., Zhong J. and Duesberg G. S., Investigation of growth-induced strain in monolayer MoS2 grown by chemical vapor deposition, *Applied Surface Science* **508** (2020) 145126.
22. Li H., Zhang Q., Yap C. C. R., Tay B. K., Edwin T. H. T., Olivier A. and Baillargeat D., From bulk to monolayer MoS2: evolution of Raman scattering, *Advanced Functional Materials* **22** (2012) 1385-1390.
23. Li S.-L., Miyazaki H., Song H., Kuramochi H., Nakaharai S. and Tsukagoshi K., Quantitative Raman spectrum and reliable thickness identification for atomic layers on insulating substrates, *ACS nano* **6** (2012) 7381-7388.
24. Falconieri M., Thermo-optical effects in Z-scan measurements using high-repetition-rate lasers, *Journal of Optics A: Pure Applied Optics* **1** (1999) 662.
25. Falconieri M. and Salvetti G., Simultaneous measurement of pure-optical and thermo-optical nonlinearities induced by high-repetition-rate, femtosecond laser pulses: application to CS2, *J Applied physics B* **69** (1999) 133-136.
26. Gnoli A., Razzari L. and Righini M., Z-scan measurements using high repetition rate lasers: how to manage thermal effects, *Optics express* **13** (2005) 7976-7981.
27. Sheik-Bahae M., Said A. A., Wei T.-H., Hagan D. J. and Van Stryland E. W., Sensitive measurement of optical nonlinearities using a single beam, *IEEE journal of quantum electronics* **26** (1990) 760-769.
28. Tsang H. K., Wong C. S., Liang T. K., Day I., Roberts S., Harpin A., Drake J. and Asghari M., Optical dispersion, two-photon absorption and self-phase modulation in silicon waveguides at 1.5 μ m wavelength, *Applied Physics Letters* **80** (2002) 416-418.
29. Zhang L., Agarwal A. M., Kimerling L. C. and Michel J., Nonlinear Group IV photonics based on silicon and germanium: from near-infrared to mid-infrared, *Nanophotonics* **3** (2014) 247-268.
30. Hon N. K., Soref R. and Jalali B., The third-order nonlinear optical coefficients of Si, Ge, and Si1− x Ge x in the midwave and longwave infrared, *Journal of Applied Physics* **110** (2011) 9.
31. Boyd R. W., *Nonlinear optics*. (Academic press, 2020).
32. Agrawal G. P., *Nonlinear fiber optics, in Nonlinear Science at the Dawn of the 21st Century*, ed.^eds. Editior (Springer, 2000), pp. Springer.